

Discovery of an Optical Jet in the BL Lac Object 3C 371^{1,2}

K. Nilsson

Tuorla Observatory, Väisäläntie 20, FIN-21500 Piikkiö, Finland

J. Heidt

Landessternwarte Heidelberg, Königstuhl, D-69117 Heidelberg, Germany

T. Pursimo, A. Sillanpää and L. O. Takalo

Tuorla Observatory, Väisäläntie 20, FIN-21500 Piikkiö, Finland

K. Jäger

Universitätssternwarte Göttingen, Geismarlandstr. 11, D-37083 Göttingen, Germany

ABSTRACT

We have detected an optical jet in the BL Lac object 3C 371 that coincides with the radio jet in this object in the central few kpc. The most notable feature is a bright optical knot 3'' (4 kpc) from the nucleus that occurs at the location where the jet apparently changes its direction by $\sim 30^\circ$. The radio, near-infrared and optical observations of this knot are consistent with a single power-law spectrum with a radio-optical spectral index $\alpha_{ro} = -0.81$. One possible scenario for the observed turn is that the jet is interacting with the material in the bridge connecting 3C 371 to nearby galaxies and the pressure gradient is deflecting the jet significantly.

Subject headings: galaxies: active — galaxies: individual (3C 371, UGC 11130)
— galaxies: jets

¹Based on observations carried out with the Nordic Optical Telescope, La Palma, Canary Islands

²Based on observations collected at the German-Spanish Astronomical Centre, Calar Alto, operated by the Max-Planck-Institut für Astronomie, Heidelberg, jointly with the Spanish National Commission for Astronomy

1. Introduction

The number of known optical counterparts of radio jets in radio galaxies and quasars has been steadily increasing during the last few years. At least seven such cases are now known (M 87, 3C 273, PKS 0521-36, 3C 66B, 3C 264, 3C 78 and 3C 120) and even more objects are suspected to harbour an optical jet (e.g. de Koff et al. 1996). In one case, 3C 66B (Fraix-Burnet 1997), optical emission has been tentatively detected also in the counterjet side. The radio emission of the jets is thought to be synchrotron radiation from relativistic electrons spiralling in the magnetic field of the jet and transporting energy to the outer lobes. At some high frequency corresponding to the highest energy electrons the spectrum cuts off and the intensity falls quickly. If this cutoff frequency is high enough, optical emission can be detected from the jet.

As the number of confirmed optical jets has increased, some patterns in their properties have emerged. In optical the jets always seem to have a “knotty” appearance and their structure in radio and optical is very similar. However, small differences in the optical and radio structures can be seen. For instance, in a detailed study of M 87, Sparks, Biretta & Macchetto (1996) found that the optical/UV emission seems to be more concentrated in the central parts of the jet and the knots show higher contrast in the optical than in the radio. Also, the radio-optical spectral index seems to be flatter in the knots than in the interknot regions. The optical jets are usually small in comparison with the radio jets that can continue tens of kiloparsecs away from the nucleus. Some optical jets display twists and/or bifurcations like the jet in 3C 264 (Crane et al. 1993).

The apparent on-sidedness of the optical jets indicates that relativistic beaming is playing an important role in modifying the intrinsic intensity distribution. If the sources with optical jets have their jets directed close to the line of sight, then these sources should be smaller than corresponding radio sources on average. Sparks et al. (1995) compared the linear sizes of a sample of 3CR radio galaxies with optical jets to those without a jet and found the radio structures of the galaxies with an optical jet to be smaller by a factor of ~ 3 . This is in accordance with the relativistic beaming picture, but intrinsic differences between the jet and counterjet cannot be ruled out yet. The optical counterjet in 3C 66B (Fraix-Burnet 1997), if confirmed, would argue for intrinsic differences between the jet and counterjet as the optical emission in the counterjet side of 3C 66B is much stronger than what is expected from relativistic beaming.

3C 371 is a nearby ($z=0.051$) BL Lac object that belongs to the 1 Jy BL Lac sample of Stickel et al. (1991). The BL Lac object is hosted by a luminous ($M_V = -22.4$) elliptical galaxy that is surrounded by a small cluster of galaxies (Stickel, Fried & Kühr 1993 and references therein). It has been mapped with the VLA at 6 cm by Wrobel & Lind (1990)

who found a dominant central core and two faint lobes east and west of the core. The eastern lobe is very diffuse with no apparent connection with the nucleus, but the western lobe is connected to the nucleus by a wiggling jet that terminates into a weak hotspot inside the lobe (see Fig. 4 [Plate 2]). Wrobel & Lind (1990) interpret this structure as an edge brightened double radio source with the angle between the source axis and line of sight large enough so that the lobes do not overlap. At the distance of ~ 3 arcsec from the nucleus the jet apparently turns $\sim 30^\circ$. At this location a sudden brightening of the jet is seen. This bright knot has been resolved by Akujor et al. (1994) at 18 cm with the MERLIN array. Their $0''.25$ resolution map shows the bright knot to be extended in the direction roughly perpendicular to the line connecting the knot and the nucleus (see Fig. 2).

2. Observations and data analysis

The R and B-band observations were carried out at the 2.56m Nordic Optical Telescope (Table 1). The pixel scales of the TEK and Loral chips were $0''.176 \text{ pix}^{-1}$ and $0''.11 \text{ pix}^{-1}$, respectively. The R-band observations of 20 Oct 1995 consist of 6×600 s exposures that have saturated the nucleus of the galaxy. In 13 Jul 1996 the individual exposures were kept between 120 and 180 seconds to avoid saturation. The B-band observations consist of 6×600 s exposures with no saturation of the nucleus. The images were de-biased and flat-fielded with IRAF using twilight flats and the individual exposures were registered and averaged. Photometric calibration of the field was achieved on the night of 17 Jun 1996 by observing standard stars from Landolt (1983,1992). The accuracy of this calibration is ~ 0.04 mag in R and ~ 0.06 mag in B. As a check of our photometry we measured a star in the 3C 371 field that is listed in the UBV calibration sequence of McGimsey & Miller (1977). For star 4 in their sequence ($B = 16.98 \pm 0.04$) we measure $B = 16.97 \pm 0.06$. This star was also used for photometric calibration of the R-band observations on 20 Oct 1995.

The K' -band observations were carried out at the Calar Alto 3.5m telescope using the MAGIC NIR camera. The pixel scale was $0''.32 \text{ pix}^{-1}$. A total of 60 frames were obtained, each consisting of 15 frames of 2 seconds each which were summed and saved. For background subtraction the exposures on target were interlaced with exposures of a field a few arcmin away from 3C 371. A total of 16 such exposures were obtained, each 15×2 seconds. The science exposures were background subtracted by the scaled median of the skyframes and scattered light and bad pixels were removed. After flat-fielding with domeflats the individual frames were registered and coadded following McLeod & Rieke (1994). Standard stars from Elias et al. (1982) were observed for photometric calibration. Although there were some thin clouds during the night, the standard stars gave consistent

results and we believe the accuracy to be much better than 0.1 mag.

To remove the light from the the host galaxy and core component in the B and R-band images we first determined the PSF from field stars and subtracted a scaled PSF at the location of the nucleus. The scaling was such that a maximum amount of light was subtracted without producing a “hole” in the underlying galaxy. The subtraction was made to facilitate later analysis by removing the diffraction spikes around the nucleus. The ISOPHOTE package in IRAF was then used to fit ellipses to the galaxy light distribution and a model galaxy image was created and subtracted from the original image. This process was iterated a few times to find and mask objects that were overlapping the 3C 371 host galaxy. The resulting residual images (Fig. 1 a,c [Plate 1]) have a background very close to zero showing that the galaxy light distribution has been succesfully modelled. Outside the nuclear region ($r > 4''$) the intensity profile first follows de Vaucouleurs profile very well, until at a radius of $\sim 13''$ (18 kpc) the profile starts to deviate from this law in the form of excess emission (see Fig. 4).

In the K' band image we do not have a bright star in the field to model and subtract the diffraction spikes. We thus proceeded directly with ellipse fitting by masking overlapping objects as previously and rejecting a fraction (8%) of highest pixels from the fit. A dark ring around the nucleus and four diffraction spikes are visible in the residual image (Fig. 1e). Also, a relatively bright object is seen $\sim 2''$ from the nucleus at $PA \sim 160^\circ$. After careful analysis of the individual K' -band images we concluded that this feature is caused by telescope movements during the 15×2 second exposures (only the sum of the 15 exposures was saved). We estimate that due to this effect about 6% of the light is moved from the center of 3C 371 to the feature $2''$ away. This also affects the K' -band photometry, but we have not made any correction for this since we are not certain of the exact amount of correction needed.

For the comparison of radio and optical images we measured the positions of 10 stars in the R-band field that can be found in the APM Northern Sky Catalogue (Irwin, Maddox & McMahon 1994) and determined the transformation from pixel positions to equatorial coordinates. Our astrometry indicates that the positions of the optical and radio nuclei agree within the positional errors that we estimate to be $0''.8$.

3. Results and discussion

Fig 1. shows a $19'' \times 19''$ field around the nucleus of 3C 371 in all three bands after removing the core and galaxy light from the images. The left panels show the “raw” images

and the right panels show the corresponding fields after 40 deconvolutions with the Lucy algorithm (Lucy 1974). Several objects can be seen to the west of the nucleus. There is clearly optical and NIR emission coming from the point where the jet apparently changes its direction and where a bright radio knot is also seen. This can be seen in Fig. 2 where we have overlaid the deconvolved best-resolution R-band image of 13 Jul 1996 with the 18 cm radio contours from Akujor et al. (1994). The knot is at a distance of $3''$ (4 kpc, $H_0 = 50 \text{ km s}^{-1} \text{ Mpc}^{-1}$) from the nucleus at PA 240° and it shows similar structure in optical as in the radio, i.e. it is extended in the direction roughly perpendicular to the jet direction. Some faint emission trailing the knot can also be seen, most notably in the B-band image. The sharp features around the nucleus in the deconvolved R and B-band images are probably artifacts caused by incomplete removal of diffraction spikes. Two faint objects are visible further out from the knot in the direction where the radio jet continues in radio maps. The one furthest out from the nucleus is consistently seen in B and R-band images at the same location. As there is no one-to-one correspondence between the radio and optical emission here, their relation to the radio jet is unclear. The outer one of these two faint objects could be one of the numerous background objects embedded in the light from 3C 371 host and the inner one is probably a noise peak amplified by the deconvolution process.

Figure 3 shows the broadband spectrum of the $3''$ knot. The radio measurements were obtained from the literature and the optical and NIR data points are from our observations. X-ray data are also available in the literature (e.g. Comastri, Molendi & Ghisellini 1995) but they are not employed here since they always refer to the total emission from 3C 371. Table 2 lists the results of our photometry. Here we have converted the K'-band flux to K-band flux using the formula by Wainscoat & Cowie (1992). The R-band flux is the average of the observations on 20 Oct 1995 and 13 Jul 1996. The errorbars in the radio are either from the original publication or if no error was given a 1σ error of 10% was assumed. In our measurements the errorbars include the errors from photon statistics and calibration, but do not include the possible error from incomplete background subtraction at the location of the objects. The radio-optical spectral index α_{ro} of the knot is -0.81 ($S_\nu \propto \nu^\alpha$) which is within the range of observed radio-optical spectral indices in jets, typically -0.9 – -0.6 (Crane et al. 1993). The spectral index in the radio domain is $\alpha_r = -0.70$ (or -0.72 if one ignores the deviant point at $\log \nu = 9.2$). Thus some steepening of the spectrum on the optical is indicated, but given the errors in Fig. 3 the observations can well be fitted with a single power-law from the radio to the optical with no indication of a break or cutoff in the spectrum.

The jet and overall radio morphology of 3C 371 bear some resemblance to those in M 87. The jet in M 87 is relatively faint until an apparent distance of $\sim 12''.5$ where a sudden brightening (knot A) is seen both in radio and optical/UV regions (e.g. Sparks, Biretta &

Macchetto 1996). Further out from the nucleus faint concentrations of emission are seen until the jet fades from visibility at a distance of $\sim 20''$. The lifetimes of the electrons emitting optical synchrotron radiation are generally too short for them to be supplied by the nucleus (\sim few hundred years in the case of M 87, see e.g. Biretta, Stern & Harris 1991) and thus some mechanism to supply fresh electrons in the hotspots is needed. Strong shocks in the jet are considered to be the most probable locations for particle acceleration. For instance, Falle & Wilson (1985) modelled the M 87 jet with a steady fluid jet to which shocks are triggered by the decreasing pressure of the interstellar medium. They interpret knot A in M 87 as location of a strong shock where a reconfinement of the jet occurs. Similar mechanism could be working in the bright $3''$ knot in 3C 371, although the appearance of both knots is more like a Mach disk and not a conical shape like in the model of Falle & Wilson (1985).

The jet in 3C 371 apparently changes direction at the location of the radio and optical knot . This property is shared only by 3C 346 that displays even more sudden bend at the location of a brightening in the optical jet (de Koff et al. 1996). If the jet in 3C 371 is relativistic at the projected distance of $3''$ from the nucleus then differences in the Doppler factor along the jet could produce apparent brightenings. An enhancement of a factor of ≥ 10 is needed in the R-band to raise the $3''$ knot from the background to the observed level. Wrobel & Lind (1990) concluded that the viewing angle θ is moderate for 3C 371. If we assume $\theta = 30^\circ$ and a Lorentz factor $\gamma = 4$ in the jet, then a 5° change in the jet direction towards the observer is sufficient. For $\gamma = 2$ and $\gamma = 1.5$ the corresponding values are 10° and 20° , respectively. Relativistic electrons moving with bulk relativistic speed in a helical jet is one possible scenario in this case. The structure seen in the radio map of Akujor et al. (1994) lends some support to this scenario, but it may not be realistic since it is not known if the electrons really move with bulk relativistic speeds in jets at a distance of ~ 4 kpc from the nucleus.

The change of direction could also be attributed to a pressure increase in the interstellar medium that diverts the jet from its original direction. This kind of redirection of the jet has been suggested to be the reason for double hotspots in the edge-brightened double radio sources (Williams & Gull 1984, 1985). The pressure increase could be supplied by the interaction of the 3C 371 host with neighboring galaxies. Figure 4 shows the 3C 371 field in the R-band after a smooth de Vaucouleurs model galaxy has been subtracted from the image. A forced de Vaucouleurs profile was used here to bring out the deviations from a smooth profile more clearly. The model was fit to the inner $r < 13''$ region which is the region reasonably well represented by de Vaucouleurs profile. Figure 4 clearly shows the bridge of emission connecting the 3C 371 host to two spiral galaxies in the SW corner of the field as noted earlier by Stickel, Fried & Kühr (1993). Their spectroscopy also shows

that the brighter of these two galaxies lies at the same redshift as the 3C 371 host. The bridge seems to continue to a distance of ~ 20 kpc from the nucleus of the 3C 371 host. We do not see the bridge to extend closer to the nucleus than this, but it is still tempting to hypothesize that gas drawn from the nearby spiral galaxies is responsible for the turn in the jet. Evidence for nonsymmetrical distribution of gas around 3C 371 nucleus was presented by Stickel, Fried & Kühr (1993) who showed that the [O III] $\lambda\lambda$ 4959,5007 emission is more extended towards the companion galaxies in the SW than towards the opposite direction. They interpreted this as a sign of tidal interaction between the 3C 371 host and the SW galaxies.

Evidence for jet interaction with the environment has been presented by previous authors both in smaller and larger scales than in 3C 371. Baum et al. (1997) presented the results of a HST and MERLIN study of 3C 264 which also exhibits an optical jet. In 3C 264 there is strong evidence for interaction between the jet and a high density circumnuclear region at 300 - 400 pc radius. Also, evidence for strong jet-cloud interaction in the quasar 3C 254 at a projected distance of ~ 15 kpc was presented by Crawford & Vanderriest (1997). The 4 kpc distance of interaction in 3C 371 is thus not unprecedented. It therefore seems, that the environmental effects can have a significant impact on jet appearance, particularly in the case of 3C 371 where the confinement of the jet probably plays a major role in the production of optical emission.

The authors thank Joan Wrobel for making the 6 cm radio image available. This work has been supported by the Academy of Finland and by the Deutsche Forschungsgemeinschaft through SFB 328 (J. Heidt) and FR 325/42-1 (K. Jäger).

Table 1. Log of observations

Date	Telescope	Band	Detector	Exposure (s)	Seeing (arcsec)
20 Oct 1995	NOT	R	TEK 1024 × 1024	3600	0.83
17 Jun 1996	NOT	B	Loral 2048 × 2048	3600	0.80
09 Jul 1996	Calar Alto 3.5m	K'	NICMOS3 256 × 256	1800	1.15
13 Jul 1996	NOT	R	TEK 1024 × 1024	1830	0.65

Table 2. Photometry of the 3'' knot.

Band	dist ''	PA °	Flux μJy
B	3.2	242	6.0 ± 0.6
R	3.0	240	11 ± 1
K	3.2	242	15^{+7}_{-5}

REFERENCES

- Akujor, C. E., Lüdke, E., Browne, I. W. A., Leahy, J. P., Garrington, S. T., Jackson, N. & Thomasson, P. 1994, *A&AS*, 105, 247
- Baum, S. A., et al. 1997, *ApJ*, in press
- Biretta, J. A., Stern, C. P. & Harris, D. E. 1991, *AJ*, 101, 1632
- Browne, I. W. A., Orr, M. J. L., Davis, R. J., Foley, A., Muxlow, T. W. B. & Thomasson, P. 1982, *MNRAS*, 198, 673
- Comastri, A., Molendi, S. & Ghisellini, G. 1995, *MNRAS*, 277, 297
- Crane, P. et al. 1993, *ApJ* 402, L37
- Crawford, C. S. & Vanderriest, C. 1997, *MNRAS*, 285, 580
- Elias, J. H., Frogel, J. A., Matthews, K. & Neugebauer, G. 1982, *AJ*, 87, 1029
- Falle, S. A. E. G. & Wilson, M. J. 1985, *MNRAS*, 216, 79
- Fraix-Burnet, D. 1997, *MNRAS*, 284, 911
- de Koff, S., Baum, S. A., Sparks, W. B., Biretta, J., Golombek, D., Macchetto, F., McCarthy, P. & Miley, G. K. 1996, *ApJS*, 107, 621
- Irwin, M., Maddox, S. & McMahon, R. 1994, *Spectrum*, 2, 14
- Landolt, A. U. 1983, *AJ*, 88, 853
- Landolt, A. U. 1992, *AJ*, 104, 340
- Lucy, L. C. 1974, *AJ*, 79, 745
- McGimsey, B. Q. & Miller, H. R. 1977, *AJ*, 82, 453
- McLeod, K. K. & Rieke, G. H. 1994, *ApJ*, 420, 58
- Pearson, T. J., Perley, R. A. & Readhead, A. C. S. 1985, *AJ*, 90, 738
- Perley, R. A., Fomalont, E. B. & Johnston, K. J. 1980, *AJ*, 85, 649
- Perley, R. A. & Johnston, K. J. 1979, *AJ*, 84, 1247
- Sparks, W. B., Biretta, J. N. & Macchetto, F. 1996, *ApJ*, 473, 254

Sparks, W. B., Golombek, D., Baum, S. A., Biretta, J., de Koff, S., Macchetto, F.,
McCarthy, P. & Miley, G. K. 1995, ApJ, 450, L55

Stickel, M., Fried, J. W. & Kühr, H. 1993, A&AS, 98, 393

Stickel, M., Padovani, P., Urry, C. M., Fried, J. W. & Kühr, H. 1991, ApJ, 374, 431

Wainscoat, R. J. & Cowie, L. L. 1992, AJ, 103, 332

Williams, A. G. & Gull, S. F. 1984, Nat, 310, 33

Williams, A. G. & Gull, S. F. 1985, Nat, 313, 34

Wrobel, J. M. & Lind, K. R. 1990, ApJ, 348, 135

Fig. 1.— A mosaic showing a $19'' \times 19''$ field around the nucleus of 3C 371 after subtraction of the core and galaxy light. The panels on the left show the “raw” images and the panels on the right the same fields after 40 deconvolutions with the Lucy algorithm. Top row (a,b) shows the B-band image, middle row (c,d) the R-band image of 13 Jul 1996 and bottom row (e,f) the K' -band image. A small cross marks the position of the optical nucleus. Light smoothing has been applied to the K' -band image. North is up and east is to the left in all panels.

Fig. 2.— The deconvolved R-band image of 13 Jul 1996 overlaid with the 18 cm radio contours of Akujor et al. (1994), used here with permission. The field size is $8''.3 \times 7''.2$, north is up and east is to the left. The arrow indicates the direction of the jet after the bright spot $3''$ from the nucleus. The tick marks are at $0.5''$ intervals.

Fig. 3.— The broadband spectrum of the knot $3''$ from the nucleus. The errorbars are 2σ errors. The fitted line has a slope of -0.81 . The radio data are from Browne et al. (1982) (408 MHz), Perley, Fomalont & Johnston (1980) (1500 MHz), Perley & Johnston (1979) (1480, 4900 MHz), Akujor et al. (1994) (1660 MHz) and Pearson, Perley & Readhead (1985) (4885 MHz). Optical and near infrared data are from this paper.

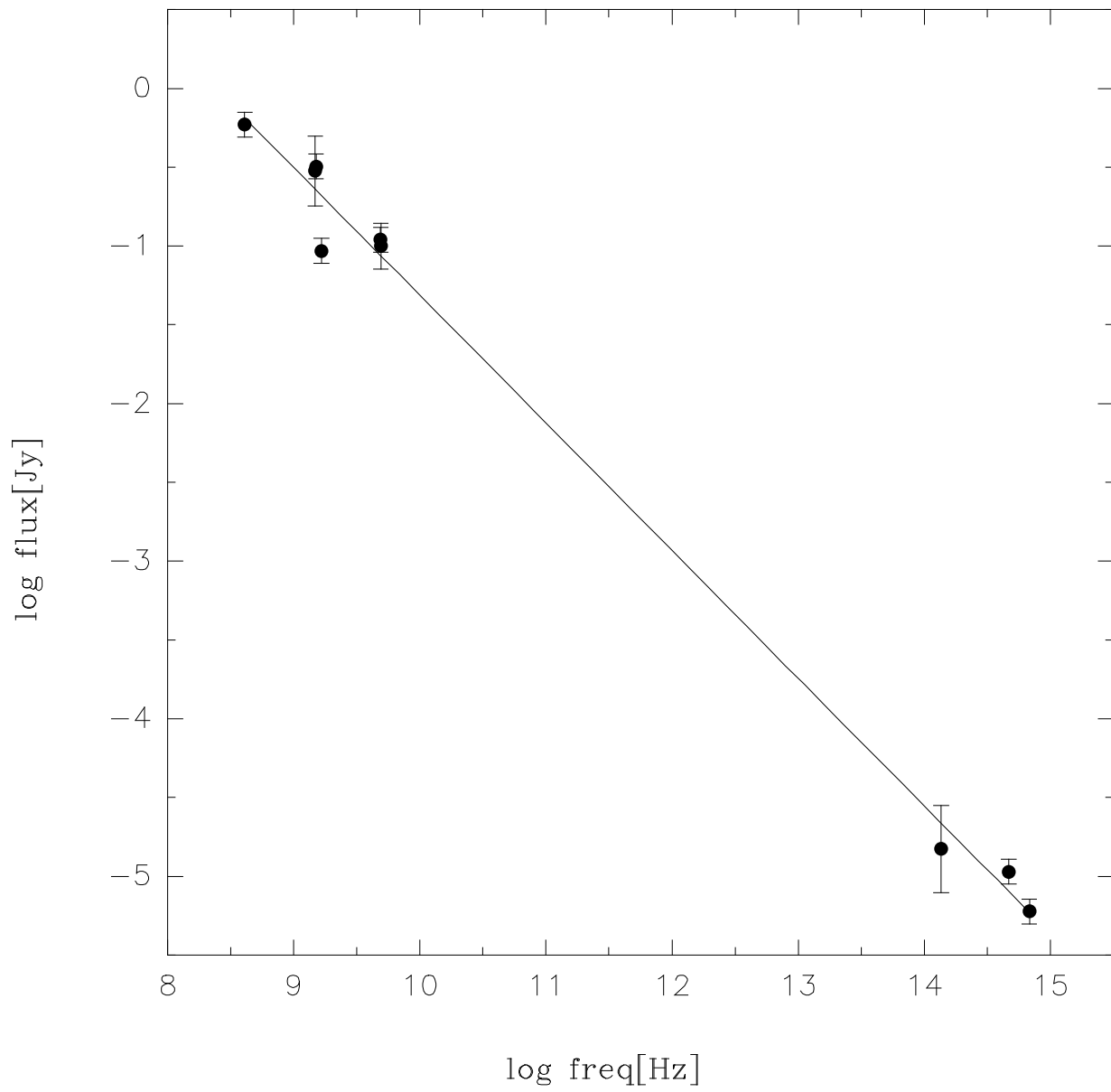
Fig. 4.— The R-band image of the field around 3C 371. The insert at the lower left corner shows the image with low contrast. In the large image a galaxy model has been subtracted as described in the text, the image has been smoothed lightly and it is shown here with high contrast to emphasize low surface brightness areas. The optical image has been overlaid by the contours of the 5 GHz radio image of Wrobel & Lind (1990). The field size is $176'' \times 159''$ and north is up and east is to the left. Note the bridge of emission connecting 3C 371 host to two spiral galaxies in the SW corner.

This figure "kanifig1.gif" is available in "gif" format from:

<http://arxiv.org/ps/astro-ph/9705179v1>

This figure "kanifig2.gif" is available in "gif" format from:

<http://arxiv.org/ps/astro-ph/9705179v1>



This figure "kanifig4.gif" is available in "gif" format from:

<http://arxiv.org/ps/astro-ph/9705179v1>